ISSN 2176-5480

22nd International Congress of Mechanical Engineering (COBEM 2013)
November 3-7, 2013, Ribeirão Preto, SP, Brazil

J-DOMINANCE IN WELDED MATERIALS WITH MECHANICAL HETEROGENEITY

Rodolfo F. de Souza
Department of Naval Architecture and Ocean Engineering, University of São Paulo, São Paulo, Brazil
rofigueira.souza@usp.br

Denis A. Ferreira
Department of Mechanical Engineering, University of São Paulo, São Paulo, Brazil
aferreira.denis@gmail.com

Claudio Ruggieri
Department of Naval Architecture and Ocean Engineering, University of São Paulo, São Paulo, Brazil
claudio.ruggieri@poli.usp.br

Abstract. *The strong dependence of crack-tip fields on specimen geometry and remote loading, particularly for moderate-to-low hardening materials under LSY conditions underlies the constraint loss pehenomenon and invalidates the one-parameter characterization of unstable cracking behavior in terms of the J-integral. Previous research efforts have enabled establishing size requirements for valid J fracture toughness testing based on the dominance of the HRR singularity which are essentially applicable to homogeneous materials. Only little effort has been expended in the past years to extend the one-parameter characterization of crack-tip conditions to welded structural components. The present work addresses the coupling effect of specimen geometry and weld strength mismatch on the crack-tip deformation limits for which J-dominance is valid in weld centerline fracture specimens. Very detailed nonlinear finite element analyses of plane-strain models for deep and shallow crack bend SE(B) and tension SE(T) fracture specimens with weld centerline cracks enable resolving the required crack-tip stress fields from which the variation of crack-tip constraint with increased values of J can be assessed. The present study provides further insight into the coupled effects of specimen geometry and weld strength mismatch on the level of deformation limit at which a one-parameter characterization of crack-tip stress fields still remains valid.*

Keywords: *J-integral, Large Scale Yielding, HRR Dominance, Centerline Weld Fracture Specimen, Clevage Fracture*

1. INTRODUCTION

Conventional fracture mechanics methodologies to assess unstable cracking behavior (stress-controlled cleavage fracture) of different cracked bodies (*i.e.*, laboratory specimens and engineering structures) rely on the similarity of their respective crack tip stress and deformation fields. Under small scale yielding (SSY) conditions, a single parameter, such as the J-integral (Rice, 1968) (or, equivalently, the crack tip opening displacement, CTOD or δ), uniquely scales the elastic-plastic near-tip fields derived by Hutchinson (Hutchinson, 1968) and Rice and Rosengren (Rice and Rosengren, 1968) for power law hardening materials which became widely known as the HRR singularity (Anderson, 2005). To the extent that such one-parameter singular fields dominate over microstructuraly significant size scales (*i.e.*, the fracture process zone of a few CTODs ahead of a macroscopic crack), the J-integral (or δ) fully describes the local conditions leading to unstable (cleavage) failure (see, *e.g.*, the review by Hutchinson (Hutchinson, 1983)).

However, the deficiencies of such one-parameter idealization become increasingly clear by examining the diverse range of crack-tip fields under extensive plastic deformation and large scale yielding (LSY) conditions, particularly in shallow crack configurations and predominantly tensile loaded structural components. The early numerical analyses of McMeeking and Parks (McMeeking and Parks, 1979) and Shih and German (Shih and German, 1981) demonstrated the strong dependence of crack-tip fields on specimen geometry and remote loading, particularly for moderate-to-low hardening materials under LSY conditions. For these materials, the interaction of crack tip plastic zones with nearby traction-free surfaces and with global plastic zones strongly affects the near tip stress-strain fields. Stresses relax below the values determined uniquely by the J-integral for the high constraint condition of small-scale yielding (SSY) which exists early in the loading of common fracture specimens (Hutchinson, 1983). This loss of a unique relationship between the crack tip fields and J underlies the constraint loss phenomenon and contributes to the observed specimen geometry and loading mode dependence on measured values of cleavage fracture toughness (J_c, CTOD) - see, *e.g.*, (Ruggieri and Dodds, 1996; Ruggieri *et al.*, 2000; Ruggieri, 2001) for illustrative cleavage fracture toughness data.

The results derived from these previous research efforts have enabled establishing size requirements for *valid* J fracture toughness testing based on the dominance of the HRR singularity which are essentially applicable to homogeneous

ISSN 2176-5480

materials. Only little effort has been expended in the past years to extend the one-parameter characterization of crack-tip conditions to welded structural components. For a given specimen geometry, mismatch between the weld metal and base plate strength affects the macroscopic mechanical behavior of the specimen in terms of its load-displacement response with a potentially strong impact on the coupling relationship between J (and, equivalently, the crack tip opening displacement, CTOD) and the near-tip stress fields. Moreover, the complex interaction between the local crack-tip fields (most often controlled by the flow properties of the weld metal) and the global plastic regime gives rise to near-tip constraint states which can differ significantly from the corresponding levels in crack-tip constraint for a homogeneous fracture specimen at the same (macroscopic) loading. In view of the technological importance of assessing fracture behavior in welded cracked structures, a more accurate evaluation of size requirements which ensure J-dominance in welded fracture specimens remains essential in more refined defect assessment procedures capable of including effects of weld strength mismatch on crack tip driving forces.

Motivated by these arguments, the present work addresses the coupling effect of specimen geometry and weld strength mismatch on the crack-tip deformation limits for which J-dominance is valid in weld centerline fracture specimens. Very detailed nonlinear finite element analyses of plane-strain models for deep and shallow crack bend SE(B) and tension SE(T) fracture specimens with weld centerline cracks enable resolving the required crack-tip stress fields from which the variation of crack-tip constraint with increased values J can be assessed. The present study provides further insight into the coupled effects of specimen geometry and weld strength mismatch on the level of deformation limit at which a one-parameter characterization of crack-tip stress fields still remains valid.

2. DESCRIPTION OF CRACK-TIP CONSTRAINT USING *SSY* FIELDS

2.1 The HRR Singularity

Development of the elastic-plastic description of Mode I, 2-D crack-tip fields for a strain hardening material begins by considering the material's uniaxial stress-strain response represented by a power law defined by the Ramberg-Osgood model in the form (Anderson, 2005)

$$\frac{\epsilon}{\epsilon_0} = \frac{\sigma}{\sigma_0} + \alpha \left(\frac{\sigma}{\sigma_0}\right)^n \tag{1}$$

where σ_0 is a reference stress, most often associated with the yield stress of the material, $\epsilon_0 = \sigma_0/E$ with E denoting the elastic (longitudinal) modulus, α is a dimensionless constant and n defines the strain hardening exponent. Generalizing the above Eq. (1) by J_2 deformation theory of plasticity (Mendelson, 1983; Chakrabarty, 2006) to a multiaxial stress state, Hutchinson (Hutchinson, 1968) and Rice and Rosengren (Rice and Rosengren, 1968) (HRR) showed that the crack-tip stress field is described by

$$\sigma_{ij} = \sigma_0 \left[\frac{EJ}{\alpha\sigma_o^2 I_n r}\right]^{1/(n+1)} \tilde{\sigma}_{ij}(n, \theta) \tag{2}$$

where (r, θ) are polar coordinates centered at the crack tip as shown in Fig. 1(a), I_n is an integration constant dependent of n only and $\tilde{\sigma}_{ij}$ represents a dimensionless constant which is a function of n and θ. Here, the J-integral defines the amplitude of the elastic-plastic singular fields thereby fully describing the conditions within a microstructurally relevant crack-tip region (with size $\approx$ 10 CTODs) as long as the above Eq. (2) is dominant.

To the extent that the crack-tip stress fields are adequately described by the HRR solution given by previous Eq. (2) and the (local) fracture process is driven by these fields over microstructurally significant size scales, there is a mechanistic rationale for correlating unstable crack propagation in two differente cracked bodies (*e.g.*, a laboratory specimen and a structural component) based on single value of J (or, equivalently, the CTOD) to characterize macroscopic loading independent of geometry and loading mode. This remarkable conclusion resulting from the HRR singularity embodies a large part of the progress achieved in elastic-plastic fracture mechanics over the past decades. However, previous analysis of the small scale yielding (SSY) problem reveals that the HRR solution does not accurately describe the crack-tip stress fields over the length scale needed to characterize the cleavage fracture process. The modified boundary layer (MBL) model described next then emerges as a more accurate and yet simple description of Mode I, 2-D crack-tip fields for a strain hardening material.

2.2 The MBL Model

The modified boundary layer (MBL) model illustrated in Fig. 1(b), originally proposed by Rice (Rice, 1967), consists of a (very large) circular region containing an edge crack and provides a convenient reference solution of an infinite body to quantify effects of finite size on the crack-tip stress fields while, at the same time, simplifying the generation of numerical solutions for stationary cracks under Mode I loading. With the plastic region limited to a small fraction of the domain radius, $R_p < R/20$ where R_p is the radius (size) of the crack-tip plastic zone, the general form of the asymptotic crack-tip stress fields well outside the plastic region is given by

ISSN 2176-5480

$$\sigma_{ij} = \frac{K_I}{\sqrt{2\pi r}} f_{ij}(\theta) \tag{3}$$

where K_I is the elastic stress intensity factor, f_{ij} define the angular variations of in-plane stress components and $(r,\ \theta)$ are polar coordinates centered at the crack tip (see Fig. 1). Numerical solutions for different levels of K_I are generated by imposing displacements of the elastic, Mode I singular field on the outer circular boundary $(r = R)$ which encloses the crack in the form

$$u\,(R,\ \theta) = \frac{K_I\,(1-\nu)}{E}\sqrt{\frac{R}{2\pi}}\cos\left(\frac{\theta}{2}\right)(3-4\nu-\cos\theta) \tag{4}$$

$$v\,(R,\ \theta) = \frac{K_I\,(1-\nu)}{E}\sqrt{\frac{R}{2\pi}}\sin\left(\frac{\theta}{2}\right)(3-4\nu-\cos\theta) \tag{5}$$

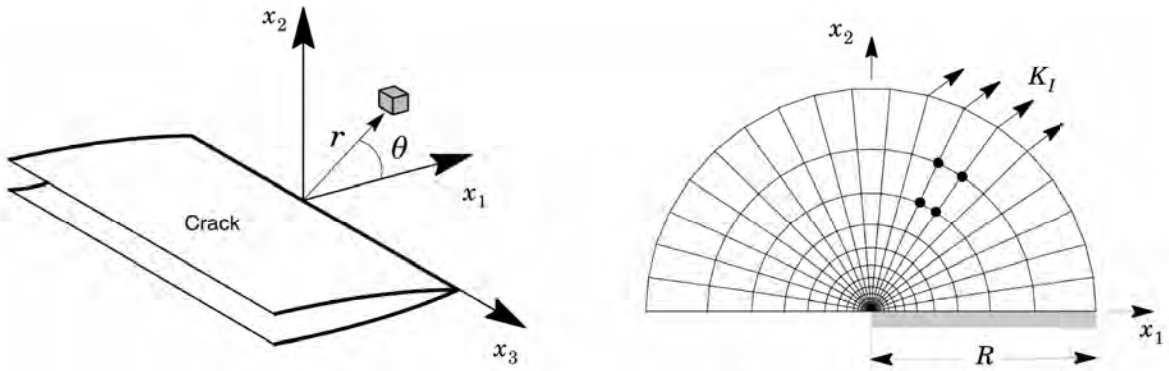

(a) (b)

Figure 1. (a) Polar coordinates centered at the crack tip; (b) Definition of the modified boundary layer (MBL) problem.

3. COMPUTATIONAL PROCEDURES AND MATERIAL MODELS

3.1 MBL Model

The modified boundary layer model previously described enables the generation of numerical solutions for stationary cracks under well-defined SSY conditions thereby providing a convenient reference solution corresponding to a high-constraint crack-tip stress fields. Figure 1(b) shows the plane-strain finite element model for an infinite domain, single-ended crack problem; Mode I loading of the far field permits analysis using one-half of the domain. A conventional mesh configuration having a focused ring of elements surrounding the crack front is employed with a small key-hole at the crack tip; the radius of the key-hole, ρ_0, is 0.0025 mm .

The plane-strain SSY analyses employ a conventional mesh configuration having a focused ring of elements surrounding the crack front. This SSY model has one thickness layer of 2065 8-node, 3-D elements with plane-strain constraints imposed $(w = 0)$ on the nodes. A small initial root radius at the crack tip (blunt tip) is employed to enhance convergence of the nonlinear iterations as presented in Fig. 2(b); the radius of the blunt tip, ρ_0, is 0.0025 mm with $R/\rho_0 = 10^6$. To limit effects of the initial root radius on the crack-tip stresses, the CTOD (δ) is required to equal four times the initial radius (ρ_0) at a deformation consistent with $(b\sigma_0/J) = 250$, where σ_0 is the reference yield stress (see Section 2.1 and b is the remaining crack ligament. This condition requires $\rho_0 = 0.0025$ mm for SSY model and flow properties considered in this work.

3.2 Fracture Specimens with Weld Centerline Crack

Nonlinear finite element analyses are described for plane-strain models of selected conventional 1-T fracture specimens (thickness $B = 25.4$ mm) with a weld centerline notch and varying geometry having a square groove weld with different weld strength mismatch. The analysis matrix includes: 1) Three-point SE(B) specimens having a/W =0.2 and 0.5 with $S/W = 4$; (2) Clamped SE(T) specimens having a/W =0.2 and 0.5 with $H/W = 6$. Here, a is the crack

ISSN 2176-5480

size, W is the specimen width, S represents the load span for the bend specimen and H denotes the distance between the clamps for the tensile specimen. The weld groove width, $2h = 15$ mm is fixed in all finite element models. Figure 2(a) shows the geometry and specimen dimensions for the analyzed crack configurations.

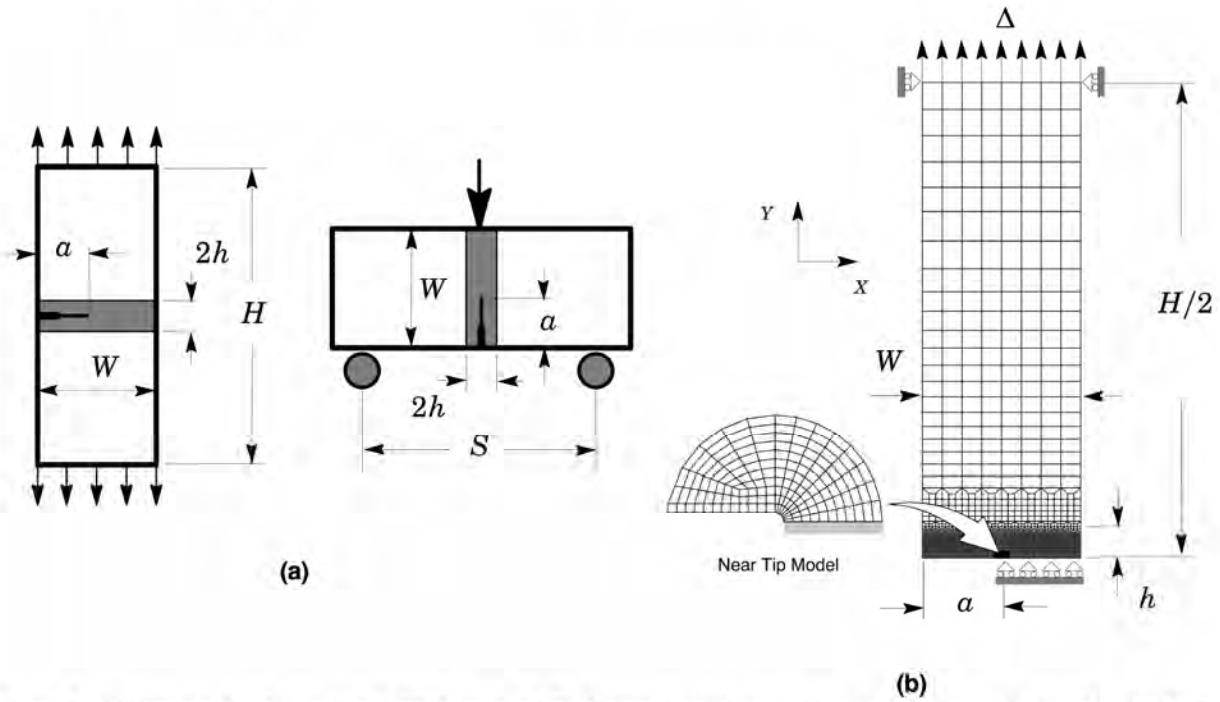

Figure 2. (a) Geometries for analyzed SE(B) and SE(T) fracture specimens with a centerline notched weld ; (b) Plane strain, finite element model having a square grooved weld with $2h = 15$ mm for the clamped SE(T) specimen with $a/W = 0.5$ and $H/W = 6$.

Figure 2(b) shows the finite element models constructed for the plane-strain analyses of the deeply-cracked, clamped SE(T) specimens with $a/W = 0.5$, $H/W = 6$ and a square-grooved, weld centerline notch with $2h = 15$ mm. The weld fracture specimen is modelled as a bimaterial component with no transition region, *i.e.*, the mechanical properties for the heat affected zone (HAZ) are not considered. All other crack models have very similar features. Again, a conventional mesh configuration having a focused ring of elements surrounding the crack front is used with a small key-hole at the crack tip; the radius of the key-hole, ρ_0, is 0.01 mm. Symmetry conditions permit modeling of only one-half of the center notch weld specimen with appropriate constraints imposed on the remaining crack ligament. A typical half-symmetric model has one thickness layer of ~3000 8-node, 3-D elements (~6400 nodes) with plane-strain constraints imposed ($w = 0$) on each node.

3.3 Material Models

The numerical solutions described here utilize an elastic-plastic constitutive model with J_2 flow theory and conventional Mises plasticity in large geometry change (LGC) setting. The welds are modelled as a bimaterial system (the heat affected zone, HAZ, is not considered in the present work) with the yield stress and hardening property of the base plate adopted as fixed in all analyses and assigned the following properties: $n = 10$ and $\sigma_0 = 412$MPa. To facilitate addressing effects of weld strength mismatch on the crack-tip stress fields, it proves convenient to define the mismatch ratio, M_y, as

$$M_y = \frac{\sigma_0^{WM}}{\sigma_0^{BM}} \tag{6}$$

where σ_0^{BM} and σ_0^{WM} denote the yield stress of the base metal and weld metal.

The finite element analyses consider material flow properties covering a relatively wide range of weld strength mismatch: evenmatch, 25% and 50% overmatch (M_y =1.0, 1.25 and 1.5), and 80% undermatch ($M_y = 0.8$). Table 1 provides the material properties utilized in the numerical analyses of the fracture specimens with square groove welds which also consider $E = 206$ GPa and $n = 0.3$. The strain hardening parameters for the weld metal are estimated from a simple correlation between the yield stress and hardening exponent applicable for typical structural steels: $n = 5$ and $E/\sigma_0 = 800$ (high hardening material), $n = 10$ and $E/\sigma_0 = 500$ (moderate hardening material), $n = 20$ and

ISSN 2176-5480

$E/\sigma_0 = 300$ (low hardening material). These ranges of properties also reflect the upward trend in yield stress with the increase in strain hardening exponent characteristic of ferritic steels. The hardening exponents for the weld metal derive by linear interpolation of the previous adopted values for E/σ_0 and n.

Table 1: Material properties adopted in the analyses for centerline weld fracture specimens with moderate hardening baseplate material ($n = 10$).

Mismatch	**Weld**		**Baseplate**	
Level	σ_0 (MPa)	n	σ_0 (MPa)	n
80% Undermatch	330	7	412	10
25% Overmatch	515	13.8	412	10
50% Overmatch	618	17.4	412	10
Homogeneous	412	10	412	10

3.4 Solution Procedures

The finite element code WARP3D (Gullerud *et al.*, 2004) provides the numerical solutions for the 3-D analyses reported here. The code solves the equilibrium equations at each iteration using a very efficient, sparse matrix solver highly tuned for Unix and PC based architectures and implements the so-called $\overline{\mathbf{B}}$ formulation (see (Gullerud *et al.*, 2004) for details) to preclude mesh lock-ups that arise as the deformation progresses into fully plastic, incompressible modes. The sparse solver significantly reduces both memory and CPU time required for solution of the linearized equations compared to conventional direct solvers.

The local value of the mechanical energy release rate at a point along the crack front is given by (Moran and Shih, 1987)

$$J = \lim_{\Gamma \to 0} \int_{\Gamma} \left[W n_1 - \sigma_{ij} \frac{\partial u_i}{\partial x_1} n_j \right] d\Gamma \tag{7}$$

where Γ denotes a contour defined in a plane normal to the front on the undeformed configuration beginning at the bottom crack face and ending on the top face, n_j is the outward normal to Γ, W denotes the stress-work density per unit of undeformed volume, σ_{ij} and u_i are Cartesian components of stress and displacement in the crack front coordinate system. The finite element computations employ a domain integral procedure (Moran and Shih, 1987) for numerical evaluation of Eq. (7) to provide pointwise values of J across the crack front at each loading level.

4. CRACK-TIP STRESS FIELDS

4.1 Reference Stress Solutions

The mechanitisc rationale for adopting plane-strain, high constraint crack-tip stress fields as the *reference* stress solution lies on the rigorous correlation between the (remote) loading transmitted to the crack tip and such fields in finite bodies when the plastic zones remain vanishingly small compared to the relevant physical dimension, *e.g.*, crack length, thickness or remaining ligament (Hutchinson, 1983). The plane-strain crack-tip fields associated with such restricted conditions are uniquely characterized by the J-integral. The HRR field described by previous Eq. (2) represents one possible reference stress solution but remains limited to idealized power-law material behavior and (nonlinear elastic) small-strain theory. In contrast, the plane-strain crack-tip fields emerging from the modified boundary layer (MBL) solution using large geometry change (LCG) assumptions describe more accurately the continuum stress and deformation fields averaged over microstructurally significant length scales while, at the same time, enabling consideration of arbitrary material flow properties without difficulties.

Figure 3(a) compares the opening mode stresses normalized by σ_0 with normalized radius, $\lambda = r/(J/\sigma_0)$, on the crack plane of the reference field obtained using (1) the HRR field, (2) a SGC boundary layer analysis and (3) a LGC boundary layer analysis. The boundary layer analyses employ a description of the material's uniaxial stress-strain response represented by previous Eq. (1) with $E/\sigma_0 = 500$, $n = 10$ and adopting $E = 206$ GPa and $\nu = 0.3$. Outside the blunting zone, the LGC and SGC stresses converge to very similar values (note that LGC values represent true stresses in the figure). Reference fields determined from SGC analyses prove adequate for most applications. However, accurate descriptions of fields near the zone of finite strains are often desirable by adopting a LGC analysis.

Figure 3(b) provides the *steady-state* reference crack-tip fields constructed for small-scale yielding (SSY) conditions with $E/\sigma_0 = 500$ and $n = 10$ ($E = 206$ GPa). In the plots, distances all scale with $(K_I/\sigma_0)^2$ whereas the opening stresses are normalized by σ_0. At very low remote loading, the near-tip stresses increase as the process of crack-tip blunting takes place. After the notch root radius increases to several times the initial radius, ρ_0, a steady state solution develops so that the near-tip fields under SSY conditions are simply a continuous series of self-similar states.

ISSN 2176-5480

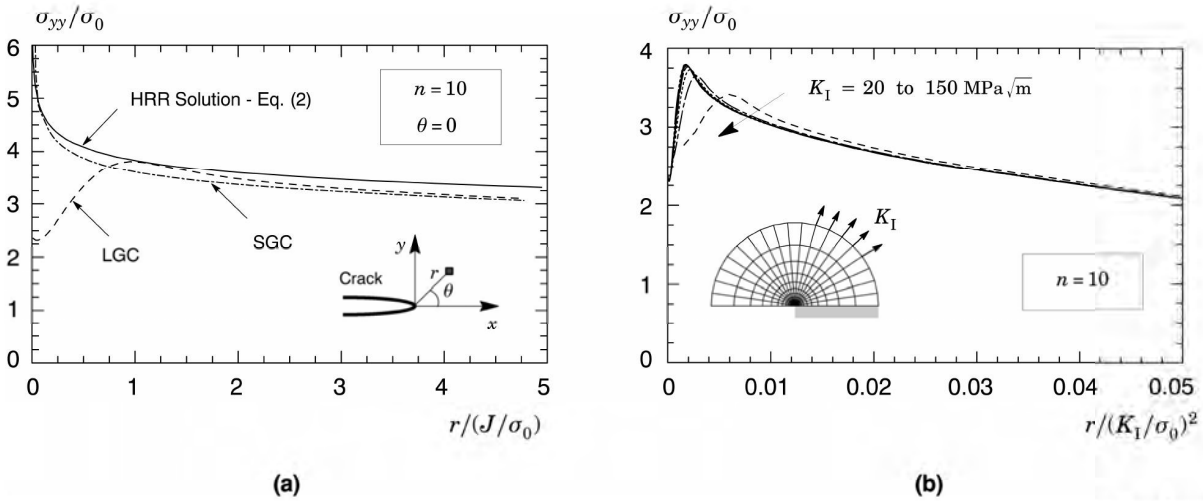

Figure 3. (a) Comparison of the HRR solution with crack-tip opening stresses for the SGC and LGC boundary analyses for $n = 10$ and $E/\sigma_0 = 500$; (b) Steady-state solution of near-tip opening stresses under SSY conditions for $n = 10$ and $E/\sigma_0 = 500$.

4.2 Evolution of Crack-Tip Stresses in Weld Centerline Fracture Specimens

Figures 4 and 5 provide typical results for the evolutions of crack-tip stresses normalized by σ_0 with nondimensional radius, $\lambda = r/(J/\sigma_0)$, for the deeply-cracked SE(B) and SE(T) configurations with two different weld strength mismatch conditions: homogeneous (evenmatch) material and 25% overmatched weld ($M_y = 1.25$ - see Eq. (6)). In all plots, the MBL reference field corresponding to each material condition is also included to enable assessment of the effect of flow properties on the boundary layer opening stresses. These results provide the difference fields needed to assess size requirements in the analyzed fracture specimens addressed next in Section 5.

Consider first the results for the SE(B) specimen with $a/W = 0.5$ displayed in Fig. 4. The near-tip stresses in the homogeneous and the welded material are in close agreement with the reference stress fields corresponding to the SSY Mode I analysis with increased deformation levels (as characterized by J in the present context) within the annulus $1 \leq r/(J/\sigma_0) \leq 2$. For $2 < r/(J/\sigma_0) \leq 5$, the near-tip finite body stresses, while falling slightly below the SSY levels, still maintain relatively good agreement with the boundary layer opening stresses even at larger J-values. Consider next the results for the SE(T) specimens with $a/W = 0.5$ shown in Fig. 5. Here, a different picture emerges as the near-tip finite body stresses deviate from the SSY solution at relatively low J-values for the entire annulus $1 \leq r/(J/\sigma_0) \leq 5$. Similar trends are also observed for the shallow crack SE(B) and SE(T) specimens with $a/W = 0.2$; to conserve space, they are omitted from the present discussion.

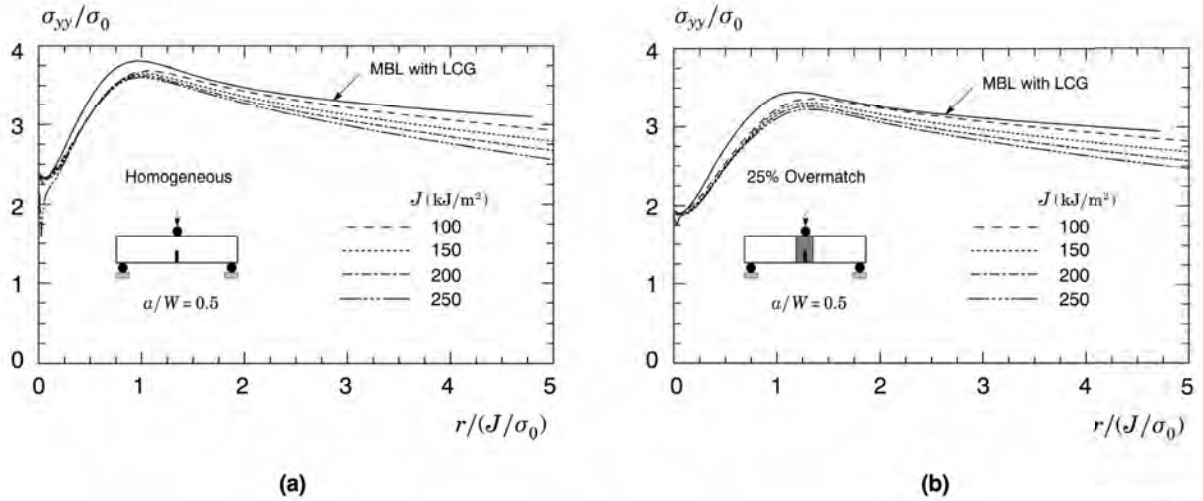

Figure 4. Evolution of near-tip opening stresses with increased J-values for the deeply-cracked SE(B) specimen: (a) Homogeneous material ($M_y = 1$); (b) 25% overmatched weld ($M_y = 1.25$).

ISSN 2176-5480

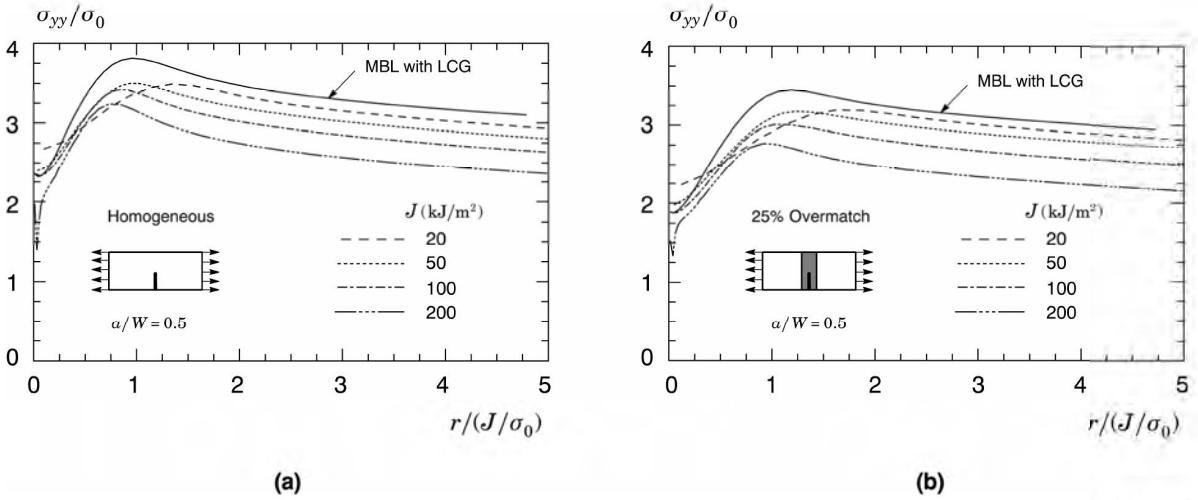

Figure 5. Evolution of near-tip opening stresses with increased J-values for the deeply-cracked SE(T) specimen: (a) Homogeneous material ($M_y = 1$); (b) 25% overmatched weld ($M_y = 1.25$).

The behavior exhibited by the tensile fracture SE(T) specimen and the shallow crack SE(B) configuration contrasts rather sharply with the evolution of opening stresses with increased J values for the deeply-cracked SE(B) specimen. Here, stresses relax below the values defined by the high constraint SSY reference field thereby underlying a severe loss of constraint for tensile specimens and shallow crack bend configurations.

5. SIZE REQUIREMENTS IN WELD CERTERLINE FRACTURE SPECIMENS

The extensive finite element analyses of weld centerline SE(B) and SE(T) fracture specimens described previously provide the basis to establish size requirements for which a one-parameter characterization of crack-tip stress fields holds true in the analyzed crack configurations. Using the SSY near-tip opening stress distribution derived from the MBL with LGC analysis as the reference field, the deformation limit defined by $M = (b\sigma_0)/J$ at which stresses in the finite body deviate by 10% of the corresponding stresses in the SSY reference field is computed for each material condition and crack configuration.

However, a key question to resolve when adopting such an approach is the proper choice of the nondimensional radius, $\lambda = r/(J/\sigma_0)$, upon which the *perturbation* in the stress field for the finite body from the SSY reference solution is measured. While outside the blunting region ($\lambda \leq 1$), where strong finite strain effects prevail so that the HRR assumptions are violated, any λ-value represents a possible choice, the present work adopts $\lambda = 4$ as a reference distance from the crack tip. A physical basis for utilizing such value derives from the relationship between J and CTOD (δ) given by (Shih, 1981)

$$J = \frac{\delta\sigma_0}{d_n} \tag{8}$$

where d_n is a constant strongly dependent of strain hardening. For a $n = 10$ material, such as the base plate material adopted here, values of d_n are in the range $0.5 \sim 0.6$, which implies that $r \approx 2\delta$ and, consequently, $\lambda \approx 4$.

Table 2 summarizes the deformation limit values, M, for each material condition and crack configuration using the procedure just outlined. The M-values for the deeply cracked SE(B) specimen agree well with previously reported values by (McMeeking and Parks, 1979) and (Shih and German, 1981). Moreover, the strong effect of specimen geometry on the deformation limit is evident in these results as parameter M ranges from 300 to $\sim$ 950 for the bend and tensile fracture specimen with shallow crack ($a/W = 0.2$), which constrasts sharply with the M-values for the high constraint, deeply-cracked SE(B) specimen. The influence of weld strength mismatch is also evident in the results displayed in Table 2. Here, increasing the levels of strength mismatch increases the J-values at which a one-parameter characterization of crack-tip stress fields, denoted J_{lim}, is still valid.

ISSN 2176-5480

Table 2: Material properties adopted in the analyses for centerline weld fracture specimens with moderate hardening baseplate material ($n = 10$).

Specimen	a/W	M_y	J_{lim} (kJ/m^2)	$M = (b\sigma_0)/J$
SE(B)	0.2	0.8	44.5	300
		1.0	43.1	388
		1.25	52.4	399
		1.5	68.5	366
SE(B)	0.5	0.8	186.7	45
		1.0	195.6	53
		1.25	202.7	65
		1.5	219.0	72
SE(T)	0.2	0.8	13.9	966
		1.0	17.7	947
		1.25	24.0	874
		1.5	31.2	804
SE(T)	0.5	0.8	83.2	101
		1.0	62.2	168
		1.25	64.4	203
		1.5	74.2	211

6. CONCLUDING REMARKS

The plane-strain finite element simulations in weld centerline fracture mechanics specimens provide quantitative results of crack-tip deformation limits for which J-Dominance is valid, considering the coupling effects of specimen geometry and weld strength mismatch. The numerical investigation described here reinforces the strong dependence of deformation limit values on specimens geometry presented in the literature. For the crack configurations analyzed, the deeply-cracked SE(B) and SE(T) specimens geometry demonstrated a better agreement with the boundary layer opening stresses when compared to the shallow-crack configurations that displayed a significant constraint loss even at lower J values.

The effects of weld strength mismatch were also studied. Results reveal that for the deeply-cracked SE(B) and SE(T) specimens, an increasing mismatch level leads to higher deformation limits values. In contrast, the shallow-cracked specimens presented a rather distinct trend in constraint loss. Both specimens have increasing deformation limits until they reach a maximum value (at $M_y = 1.25$) from which it begins to decrease, suggesting the existence of a point where overmatch effects tend to diminish.

On going work focuses in investigate the effects of weld strength mismatch in a wider range of materials, fracture specimens configurations and weld groove widths in order to extend the limit deformation results.

7. ACKNOWLEDGMENTS

This investigation is supported by Fundacao de Amparo a Pesquisa do Estado de Sao Paulo (FAPESP) through grant 2009/54229-3. The work of CR is also supported by the Brazilian Council for Scientific and Technological Development (CNPq) through Grants 304132/2009-8 and 476581/2009-5.

8. REFERENCES

Anderson, T.L., 2005. *Fracture Mechanics: Fundaments and Applications - 3rd Edition*. CRC Press, Boca Raton, FL.

Chakrabarty, J., 2006. *Theory of Plasticity*. Elsevier Butterworth-Heinemann, Oxford, UK, 3rd edition.

Gullerud, A., Koppenhoefer, K., Roy, A., RoyChowdhury, S., Walters, M., Bichon, B., Cochran, K. and Dodds, R.H., 2004. "WARP3D: Dynamic nonlinear fracture analysis of solids using a parallel computers and workstations". Structural Research Series (SRS 607) UILU-ENG-95-2012, University of Illinois at Urbana-Champaign.

Hutchinson, J.W., 1968. "Singular behavior at the end of a tensile crack in a hardening material". *Journal of the Mechanics and Physics of Solids*, Vol. 16, pp. 13–31.

Hutchinson, J.W., 1983. "Fundamentals of the phenomenological theory of nonlinear fracture mechanics". *Journal of Applied Mechanics*, Vol. 50, pp. 1042–1051.

McMeeking, R.M. and Parks, D.M., 1979. "On criteria for j-dominance of crack-tip fields in large-scale yielding". In J.D. Landes, J.A. Begley and G.A. Clarke, eds., *Elastic-Plastic Fracture*. American Society for Testing and Materials, Philadelphia, ASTM STP 668, pp. 175–194.

Mendelson, A., 1983. *Plasticity: Theory and Applications - 2nd Edition*. Krieger Publishing.

ISSN 2176-5480

Moran, B. and Shih, C.F., 1987. "A general treatment of crack tip contour integrals". *International Journal of Fracture*, Vol. 35, pp. 295–310.

Rice, J.R., 1967. "Mechanics of crack tip deformation and extension by fatigue". In J. Grosskreutz, ed., *Fatigue Crack Propagation*. American Society for Testing and Materials, Philadelphia, ASTM STP 415, pp. 247–311.

Rice, J.R., 1968. "A path independent integral and the approximate analysis of strain concentration by notches and cracks". *Journal of Applied Mechanics*, Vol. 35, pp. 379–386.

Rice, J.R. and Rosengren, G.F., 1968. "Plane strain deformation near a crack tip in a power-law hardening material". *Journal of the Mechanics and Physics of Solids*, Vol. 16, pp. 1–12.

Ruggieri, C., 2001. "Influence of threshold parameters on cleavage fracture predictions using the Weibull stress model". *International Journal of Fracture*, Vol. 110, pp. 281–304.

Ruggieri, C. and Dodds, R.H., 1996. "A transferability model for brittle fracture including constraint and ductile tearing effects: A probabilistic approach". *International Journal of Fracture*, Vol. 79, pp. 309–340.

Ruggieri, C., Gao, X. and Dodds, R.H., 2000. "Transferability of elastic-plastic fracture toughness using the Weibull stress approach: Significance of parameter calibration". *Engineering Fracture Mechanics*, Vol. 67, pp. 101–117.

Shih, C.F., 1981. "Relationship between the j-integral and the crack opening displacement for stationary and extending cracks". *Journal of the Mechanics and Physics of Solids*, Vol. 29, pp. 305–326.

Shih, C.F. and German, M.D., 1981. "Requirements for a one-parameter characterization of crack tip fields by the hrr singularity". *International Journal of Fracture*, Vol. 17, pp. 27–43.

9. RESPONSIBILITY NOTICE

The authors are the only responsible for the printed material included in this paper.